Geoscience Frontiers 12 (2021) 147–160

HOSTED BY

Contents lists available at ScienceDirect

Geoscience Frontiers

journal homepage: www.elsevier.com/locate/gsf

Research Paper

Adakite-like granitoids of Songkultau: A relic of juvenile Cambrian arc in Kyrgyz Tien Shan

D. Konopelko [a,b,*], R. Seltmann [c], A. Dolgopolova [c], I. Safonova [b,d], S. Glorie [e], J. De Grave [f], M. Sun [g]

[a] St. Petersburg State University, 7/9 University Embankment, St. Petersburg, 199034, Russia
[b] Novosibirsk State University, 1 Pirogova St., Novosibirsk, 630090, Russia
[c] Natural History Museum, Centre for Russian and Central EurAsian Mineral Studies (CERCAMS), London, SW7 5BD, UK
[d] Sobolev Institute of Geology and Mineralogy SB RAS, Koptyuga Ave. 3, Novosibirsk, 630090, Russia
[e] Department of Earth Sciences, School of Physical Sciences, The University of Adelaide, SA, 5005, Australia
[f] Department of Geology, Ghent University, Krijgslaan 281/S8, B-9000, Ghent, Belgium
[g] Department of Earth Sciences, The University of Hong Kong, Pokfulam Road, Hong Kong, China

ARTICLE INFO

Handling Editor: Sanghoon Kwon

Keywords:
Northern Tien Shan (Tianshan)
Terskey suture
Adakite
Cambrian juvenile arc

ABSTRACT

The early Paleozoic Terskey Suture zone, located in the southern part of the Northern Tien Shan domain in Kyrgyzstan, comprises tectonic slivers of dismembered ophiolites and associated primitive volcanics and deep-marine sediments. In the Lake Songkul area, early-middle Cambrian pillow basalts are crosscut by the Songkultau intrusion of coarse-grained gneissose quartz diorites and tonalites with geochemical characteristics typical for high-SiO_2 adakites (SiO_2 > 56 wt.%, Al_2O_3 > 15 wt.%, Na_2O > 3.5 wt.% and high Sr/Y and La/Yb ratios). The Songkultau granitoids have positive initial ε_{Nd} (+3.8 to +6.4) and ε_{Hf} (+12.3 to +13.5) values indicating derivation from sources with MORB-like isotopic signature. Volcanic formations, surrounding the Songkultau intrusion, have geochemical affinities varying from ocean floor to island arc series. This rock assemblage is interpreted as a relic of an early–middle Cambrian primitive arc where the adakite-like granitoids were derived from partial melting of young and hot subducted oceanic crust. An age of 505 Ma, obtained for the Songkultau intrusion, shows that hot subduction under the Northern Tien Shan continued until middle Cambrian. The primitive arc complexes were obducted onto the Northern Tien Shan domain, where the Andean type continental magmatic arc developed in Cambrian and Ordovician. Formation of the Andean type arc was accompanied by uplift, erosion and deposition of coarse clastic sediments. A depositional age of ca. 470 Ma, obtained for the gravellites in the Lake Songkul area, is in agreement with the timing of deposition for lower Ordovician conglomerates elsewhere in the Northern Tien Shan, and corresponds to the main phase of the Andean type magmatism. The Songkultau adakites in association with surrounding ocean floor and island arc formations constitute a relic of a primitive Cambrian arc and represent a juvenile domain of substantial size identified so far within the predominantly crustal-derived terranes of Tien Shan. On a regional scale this primitive arc can be compared with juvenile Cambrian arcs of Kazakhstan, Gorny Altai and Mongolia.

1. Introduction

The Central Asian Orogenic Belt (CAOB) is one of the largest accretionary orogens on Earth that formed by continuous accretion of terranes from Neoproterozoic to late Paleozoic (Zonenshain et al., 1990; Şengör et al., 1993; Windley et al., 2007; Burtman, 2010; Xiao et al., 2013). During the last decades several large domains containing significant amounts of juvenile crust have been recognized in the CAOB, which lead some authors to postulate unusually high juvenile crust production rates in the CAOB during the Paleozoic (Jahn et al., 2000; Jahn, 2004; Wang et al., 2009). Although the theory of anomalously high crustal growth in the CAOB was recently disputed (Kröner et al., 2014, 2017), it is generally accepted that large domains of the juvenile crust occur in NE Kazakhstan and Junggar, in the Altai-Sayan

* Corresponding author. St. Petersburg State University, 7/9 University Embankment, St. Petersburg, 199034, Russia.
E-mail addresses: konopelko@inbox.ru, konopelko@gmail.com (D. Konopelko).
Peer-review under responsibility of China University of Geosciences (Beijing).

https://doi.org/10.1016/j.gsf.2020.08.006
Received 5 December 2019; Received in revised form 24 June 2020; Accepted 13 August 2020
Available online 1 September 2020

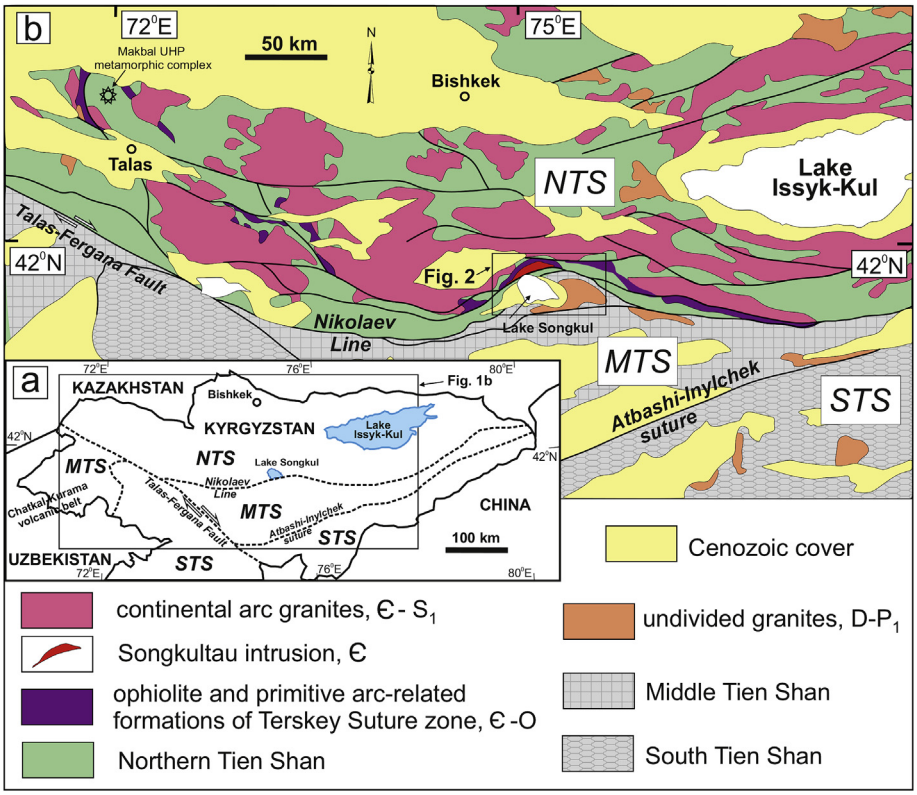

Fig. 1. (a) Principal tectonic units of Tien Shan in Kyrgyzstan; (b) schematic geological map of the Northern Tien Shan showing distribution of early Paleozoic continental arc granites and ophiolitic and arc-related formations of the Terskey Suture zone (based on Alekseiev et al., 2019, modified by the authors). Abbreviations: NTS – Northern Tien Shan, MTS – Middle Tien Shan, STS – Southern Tien Shan.

region of Siberia and in the Lake and Trans-Altai zones of Mongolia, while a broad belt stretching from NW Kazakhstan via the Uzbek and Kyrgyz Tien Shan to NW China formed on older continental crust (Kröner et al., 2017).

In this paper we present (i) new SHRIMP zircon U–Pb age, (ii) whole rock Nd data and (iii) Hf-in-zircon data for a rare example of a mantle-derived granitoid suite from the predominantly crustal Kyrgyz Tien Shan. Contrastingly juvenile isotopic compositions for the Cambrian Songkultau granites were originally recognized within the frame of a larger Sr-Nd-Hf isotopic mapping project (Seltmann et al., 2008), which lead us to conduct additional investigations that resulted in the recognition of a relic primitive arc complex with adakite geochemical affinity. The obtained results confirm Cambrian age of the Songkultau intrusion and characterize the geochemistry of the Songkultau granitoids and associated volcanic and sedimentary formations. These data have important implications for deciphering the early Paleozoic history of the Kyrgyz Northern Tien Shan where Cambro–Ordovician formations remain poorly studied due to lack of geochemical and geochronological data. In addition, conventional stratigraphic correlation of these early Paleozoic suites is difficult as they do not contain datable fossils and occur in relatively small, disconnected and often metamorphosed tectonic blocks. On a regional scale, a primitive Cambrian arc recognized in the Northern Tien Shan, belongs to a system of the early Paleozoic juvenile arcs, which are described in adjacent areas of the CAOB in Chinese Tien Shan (Gao et al., 2009; Ma et al., 2013; Wang et al., 2015), Kazakhstan (Ryazantsev et al., 2009; Degtyarev, 2012; Liu et al., 2016; Safonova et al., 2017), Gorny Altai (Buslov et al., 2002) and Mongolia (Janoušek et al., 2018). Analysis of these oldest in CAOB arc systems is a powerful tool to delineate the ancient convergent continental margins and associated accretionary complexes, and the here presented data on the Northern Tien Shan arc provide important clues for further understanding the overall tectonic architecture of the southwestern CAOB.

2. Geological setting of Songkultau intrusion, previous work and sampling

The Tien Shan orogen, located in the southwestern part of the CAOB, was formed in several stages of subduction–accretion with two major episodes comprising the early Paleozoic (Caledonian) and the late Paleozoic (Hercynian) collisional orogenic events and subsequent reactivation of the region during the Mesozoic and Cenozoic (Windley et al., 2007; Biske and Seltmann, 2010; Xiao et al., 2013; Kröner et al., 2014; Jepson et al., 2018). The Kyrgyz part of Tien Shan is traditionally divided into three major tectonic zones or domains: the Northern Tien Shan (NTS), the Middle Tien Shan (MTS) and the South Tien Shan (STS) (Zonenshain et al., 1990; Biske and Seltmann, 2010; Burtman, 2015). These E–W trending linear zones are cut by the NW trending Talas-Fergana Fault with a total dextral offset of about 200 km (Fig. 1a). The NTS is represented by an early Paleozoic continental arc, built up on Precambrian basement as a result of northward subduction and subsequent closure of the Terskey Ocean, a branch of the Palaeo-Asian Ocean, during the middle Ordovician (Lomize et al., 1997; Ghes, 2008). The main component of the MTS is the Chatkal-Kurama volcano-plutonic belt that formed during the evolution and closure of the Turkestan Ocean to the south. The late Paleozoic Chatkal-Kurama continental arc formed on the MTS basement, which represents a Precambrian microcontinent and Ordovician continental arc terranes welded together in the late Ordovician (Alexeiev et al., 2016; Konopelko et al., 2017). The STS represents a pile of folded tectonic nappes, which are thrust southward upon the passive margin of the Karakum-Tarim continent during closure of the Turkestan Ocean in the late Carboniferous (Biske and Seltmann, 2010;

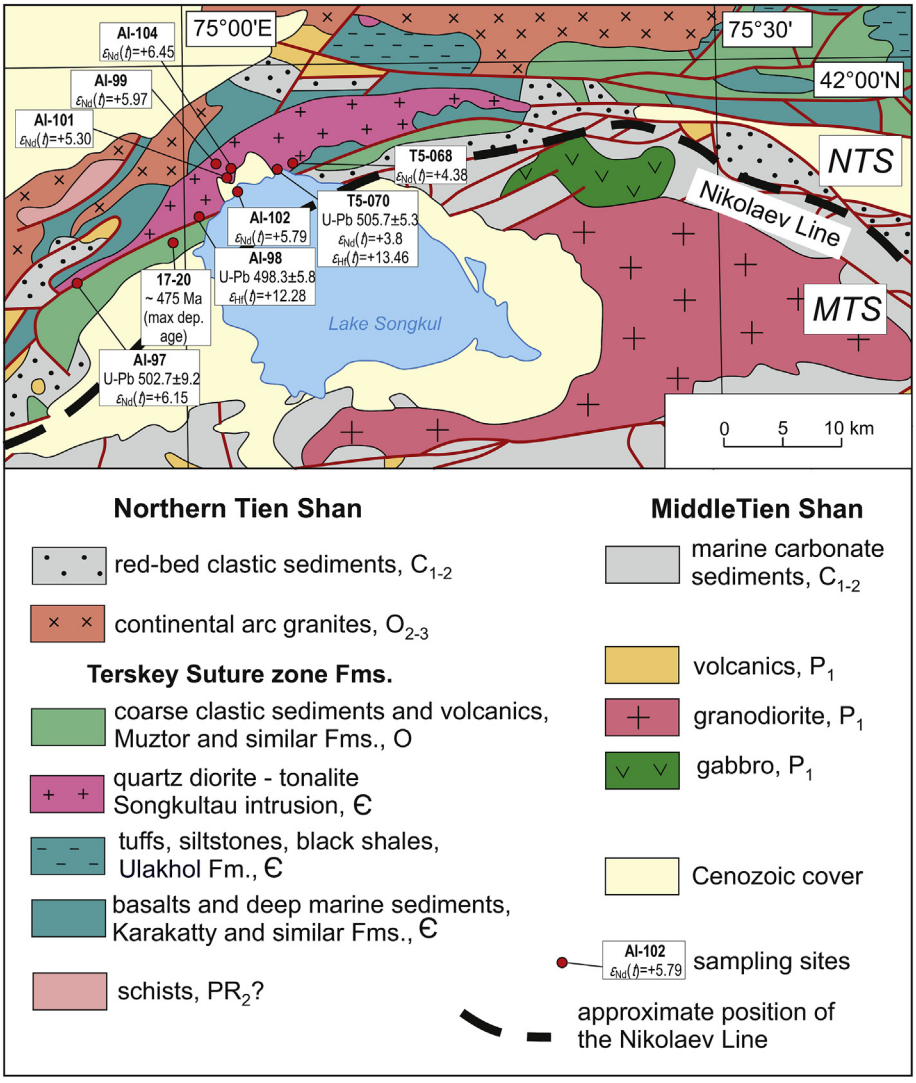

Fig. 2. Simplified geological map of Lake Songkul area and sampling sites (based on 1:500,000 map of Tursungaziev and Petrov (2008), modified by the authors). Abbreviations: NTS – Northern Tien Shan, MTS – Middle Tien Shan.

Burtman, 2015; Konopelko et al., 2019 and references therein).

The NTS is built up on Precambrian basement consisting of Mesoproterozoic metasediments intruded by ca. 1.15–1.05 Ga granites, which were derived from Paleoproterozoic or older crust as evidenced by their Nd and Hf model ages (Bakirov and Maksumova, 2001; Kiselev and Maksumova, 2001; Kröner et al., 2013). Further evolution of the NTS was controlled by the development of the Terskey Ocean to the south and the transformation of the NTS in its Andean type northern active margin. The beginning of this process is marked by Cambrian continental arc magmatism and by Cambrian–early Ordovician ophiolites preserved in the Terskey Suture zone (Lomize et al., 1997; Mikolaichuk et al., 1997; Kiselev, 1999; Kiselev and Maksumova, 2001; Alexeiev et al., 2019). Progressive subduction to the north and subsequent accretion of the MTS to the NTS during closure of the Terskey Ocean in the middle Ordovician resulted in continuous Andean type magmatism, during which voluminous subduction-related and collisional Ordovician–early Silurian granitoids were emplaced (Fig. 1b) (Kiselev and Maksumova, 2001; Ghes, 2008; Konopelko et al., 2008). After the middle Ordovician collision the NTS and MTS developed as parts of the Paleo-Kazakhstan continent and were later affected by the early Devonian intraplate and the early Permian post-collisional magmatism (Konopelko et al., 2008; Seltmann et al., 2011).

The strip of ophiolitic fragments, defined as the Ordovician Terskey Suture (Lomize et al., 1997; Mikolaichuk et al., 1997; Ghes, 2008; Degtyarev et al., 2013), is bound to the southern margin of the NTS domain (Fig. 1b). In the Lake Songkul area the Terskey Suture zone is parallel to the Nikolaev Line, which was recognized in the 1930s as a regional tectonic lineament separating the NTS and MTS domains (Nikolaev, 1933; Popov, 1938) (Figs. 1–3). The Nikolaev Line represents a combination of late Carboniferous top-to-the north thrusts and Permian strike-slip faults separating the early Paleozoic (Caledonian) orogen of the Northern Tien Shan to the north and the late Paleozoic (Hercynian) formations of the Middle Tien Shan to the south (Alexeiev et al., 2017 and references therein).

Paleontological ages of sedimentary sequences in the Terskey Suture zone ophiolites range from early Cambrian to early Ordovician (Mikolaichuk et al., 1997) with only few published complementary zircon U–Pb ages in the range of 518–516 Ma (Qian et al., 2009; Degtyarev et al., 2013). Around and east of Lake Songkul, the Terskey Suture ophiolites are represented by pillow basalts and associated rocks of the Karakatty, Bel'tepshi and Sultansary Fms. (Fig. 2) (Osmonbetov, 1982; Tursungaziev and Petrov, 2008). The rocks of these formations do not contain datable fossils and their early Cambrian age was assumed based on their stratigraphic position below other fossiliferous strata (Maksumova et al., 1988; Mikolaichuk et al., 1997). A supra-subduction origin of the volcanic rocks in the Bel'tepshi and Sultansary Fms. was first

suggested by Mikolaichuk et al. (1997) and later confirmed by Alexeiev et al. (2019) based on geochemical data (low La/Yb ratios, negative Nb–Ta anomalies and positive $\varepsilon_{Nd}(t)$ values). Similar supra-subduction setting was suggested for younger ophiolites with late Cambrian–early Ordovician ages (Demina et al., 1995; Ghes, 2008; Alexeiev et al., 2019), which were virtually coeval with the initiation of continental subduction-related granitoid magmatism (Konopelko et al., 2008, 2014; Alexeiev et al., 2019) but formed in a deeper marine setting, based on occurrences of pillow lava and deep-marine turbidite and chert interlayers in volcanic rocks (Alexeiev et al., 2019). The evolution of the Terskey Ocean is further constrained by ages of UHP eclogite-facies metamorphic rocks, representing marginal parts of the NTS microcontinent involved in the subduction. The ages of the HP-UHP metamorphic events in the Makbal complex, located in the western part of the Terskey suture zone (Fig. 1b), are constrained within 510–475 Ma (Tagiri et al., 1995; Konopelko and Klemd, 2016) with the oldest ages indicating ongoing subduction in the early–middle Cambrian.

The study area is located in the Songkultau Mountains on the west shore of Lake Songkul. The main geological features of the area include the Songkultau massif of diorites and quartz diorites which crosscut pillow basalts of the Karakatty Fm., and are tectonically juxtaposed with the Muztor Fm. consisting of coarse clastic sediments with thick conglomerate layers (Tursungaziev and Petrov, 2008) (Fig. 2). These Cambrian–Ordovician formations constitute one of the ophiolite slivers immediately north of the Nikolaev Line that strikes along the northern shore of Lake Songkul and separates the NTS domain from the MTS located to the south (Figs. 1 and 2). In this area the Nikolaev Line corresponds to the front of the top-to-the north low angle overthrusts, which thrust open marine Carboniferous limestones of the MTS on the Serpukhovian to Bashkirian red beds of the NTS (Fig. 2). The Karakatty Fm., as well as the similar Bel'tepshi and Sultansary Fms., consisting of pillow basalts intercalated with deep-marine sediments, are shown on regional geological maps as early Cambrian (Osmonbetov, 1982; Tursungaziev and Petrov, 2008). The Songkultau massif of diorites and quartz diorites is shown on maps as early Ordovician (Osmonbetov, 1982; Tursungaziev and Petrov, 2008), however recent zircon U–Pb dating revealed ages in the range of 503–498 Ma corresponding to the middle–late Cambrian (De Grave et al., 2011).

Despite the progress with zircon dating, the geochemical affinity of the Songkultau granitoids and surrounding basalts remained poorly studied and, therefore, additional sampling and analysis of previously geochronologically investigated granitoid samples (De Grave et al., 2011) was undertaken. Surrounding basalts of the Karakatty Fm. were sampled along the southern contact of the intrusion and on the northern shore of Lake Songkul. The obtained results on these samples are discussed below in combination with published geochemical data on similar volcanic formations of the area. Lower Paleozoic clastic sediments in the vicinity of the Songkultau intrusion are represented by the Muztor Fm. shown on maps as middle Ordovician (Tursungaziev and Petrov, 2008). The contact between the Muztor sediments and the Songkultau rocks is shown on geological maps as tectonic (Fig. 2). However basal conglomerates in the bottom of the Muztor Fm., unconformably overlying the basalts of the Karakatty Fm., were described in adjacent areas (Dzhenchuraeva et al., 2015). The Muztor Fm. was investigated in the southwestern part of the study area (Fig. 2) where it consists of thick boulder conglomerates with cobbles mainly represented by mafic volcanics and minor granitoids similar to those of the Songkultau intrusion (Fig. 3d). The conglomerates are intercalated with more sandy layers, from which a gravellite sample was collected for detrital zircon study.

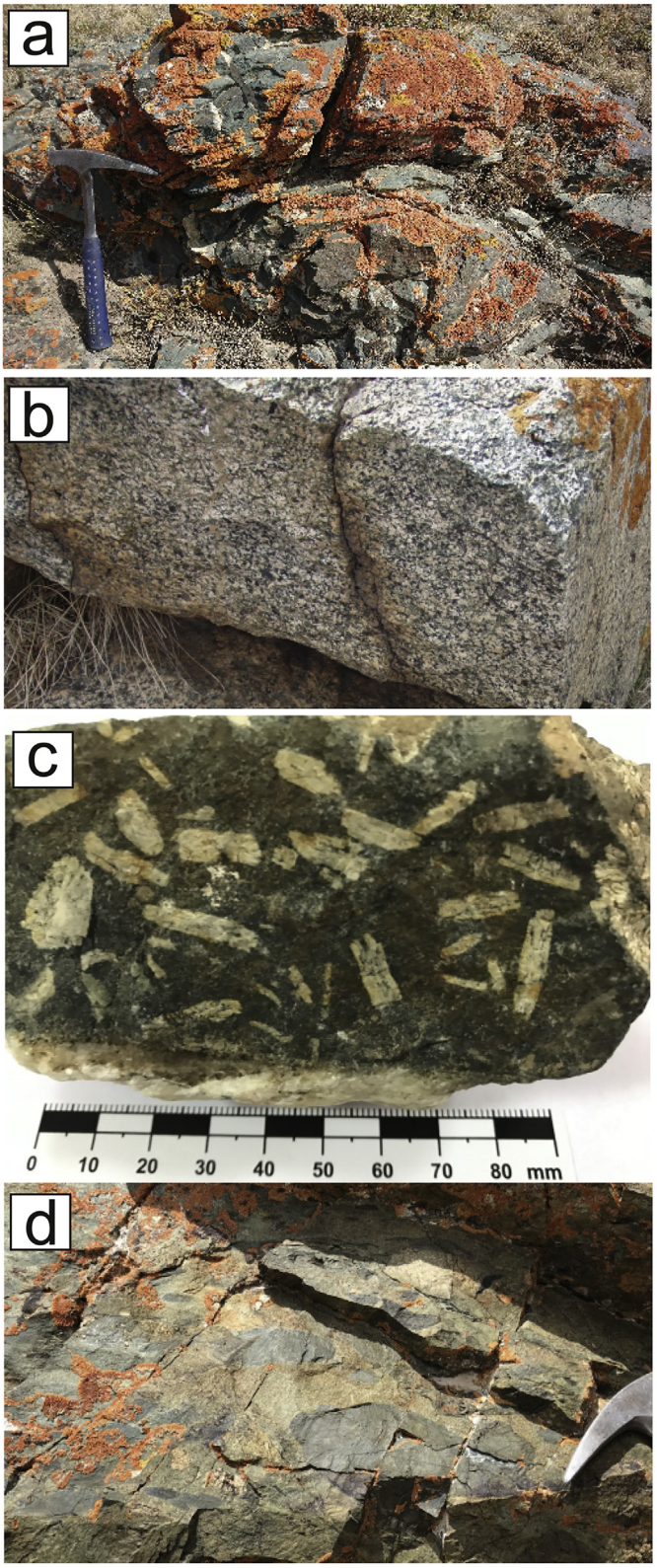

Fig. 3. Outcrop and sample photographs of rocks from Lake Songkul area: (a) pillow basalts of the Karakatty Fm. from the north shore of Lake Songkul (sample 17-14), (b) typical coarse-grained quartz diorite, (c) quartz diorite porphyry from endocontact zone, (d) conglomerate of the Muztor Fm.

3. Results

We provide a geochemical dataset (including whole rock Nd and Hf-in-zircon data) from the Songkultau intrusion and surrounding basaltic formations, as well as additional SHRIMP zircon age data for the Songkultau quartz diorite and ages of detrital zircons from gravellite of the

Table 1
Description of samples and summary of results.

Sample No.	Rock-type and Fm./suite	Coordinates WGS-84	Summary of results					
			U–Pb age (Ma)	$\varepsilon_{Nd}(t)$	T_{DM} (Ga)	T_{DM}* (Ga)	$\varepsilon_{Hf}(t)$[a]	t_{Hf}[a] (Ga)
17-20	Gravellite of Muztor Fm.	N 41°52′26″ E 75°59′21″	~475 (max dep. age)	n.a.	n.a.	n.a.	n.a.	n.a.
T5-070	Diorite of Songkultau intr.	N 41°55′32″ E 75°05′14″	505.7 ± 5.3	+3.8	0.96	0.89	+13.46	0.62
T5-068	Diorite of Songkultau intr.	N 41°55′39″ E 75°06′45″	n.a.	+4.4	0.95	0.88	n.a.	n.a.
AI-98	Diorite of Songkultau intr.	N 41°53′06″ E 75°01′05″	498.3 ± 5.8[b]	n.a.	n.a.	n.a.	+12.28	0.65
AI-101	Diorite of Songkultau intr.	N 41°55′08″ E 75°02′21″	n.a.	+5.3	0.92	0.80	n.a.	n.a.
AI-102	Diorite of Songkultau intr.	N 41°54′36″ E 75°02′48″	n.a.	+5.8	0.80	0.76	n.a.	n.a.
AI-97	Diorite of Songkultau intr.	N 41°50′37″ E 74°54′04″	502.7 ± 9.2[b]	+6.2	0.78	0.73	n.a.	n.a.
AI-99	Diorite of Songkultau intr.	N 41°55′56″ E 75°01′44″	n.a.	+6.0	0.72	0.75	n.a.	n.a.
AI-104	Diorite of Songkultau intr.	N 41°55′08″ E 75°02′21″	n.a.	+6.4	0.84	0.71	n.a.	n.a.
A1437b[c]	Andesite of Sultansary Fm.	N 41°46′06″ E 76°15′56″	~525 (?)	+3.7[c]	n.a.	n.a.	n.a.	n.a.
A1439a[c]	Basalt of Bel'tepshi Fm.	N 41°46′36″ E 76°18′06″	~530 (?)	+5.3[c]	n.a.	n.a.	n.a.	n.a.

n.a. – not analyzed or not calculated.
[a] Mean values.
[b] After De Grave et al. (2011).
[c] After Alexeiev et al. (2019); Nd model ages were not calculated for samples A1439a and A1437b due to their high $^{147}Sm/^{144}Nd$ ratio (<0.14).

Muztor Fm. Sampling sites of geochronologically investigated samples are shown in Fig. 2 and their coordinates together with a summary of the results are listed in Table 1. Description and coordinates of the samples retained for geochemical analysis are given in Supplementary Table S1. Outcrop photographs of representative rock-types from the Songkultau area are shown in Fig. 3. Detailed descriptions of the applied methods and analytical procedures are given in the Supplementary Material S2.

3.1. Petrography and geochemistry

The Songkultau intrusion makes up an elongate body (50 km long and 0.5–6 km wide) that was emplaced into basalts and deep-marine sediments of the Karakatty Fm. (Fig. 2). The intrusion is composed of relatively homogeneous coarse-grained gneissose quartz diorites and tonalites consisting of plagioclase (oligoclase-andesine 55%–60%), amphibole (15%–25%), quartz (5%–20%) and minor K-feldspar (0.5%–3%) (Figs. 3b and 4c–e). Accessory minerals are represented by apatite, titanite, zircon and allanite. In the QAPF diagram, the modal mineral compositions of the rocks plot in the fields of quartz-diorite and tonalite (not shown). The Songkultau granitoids crosscut surrounding basalts of the Karakatty Fm. with pronounced marginal endocontact zones of porphyritic varieties, indicating a shallow emplacement level (Figs. 3c and 4f). The majority of samples are strongly altered with replacement of amphibole by chlorite and plagioclase by saussurite (Fig. 4c), which is

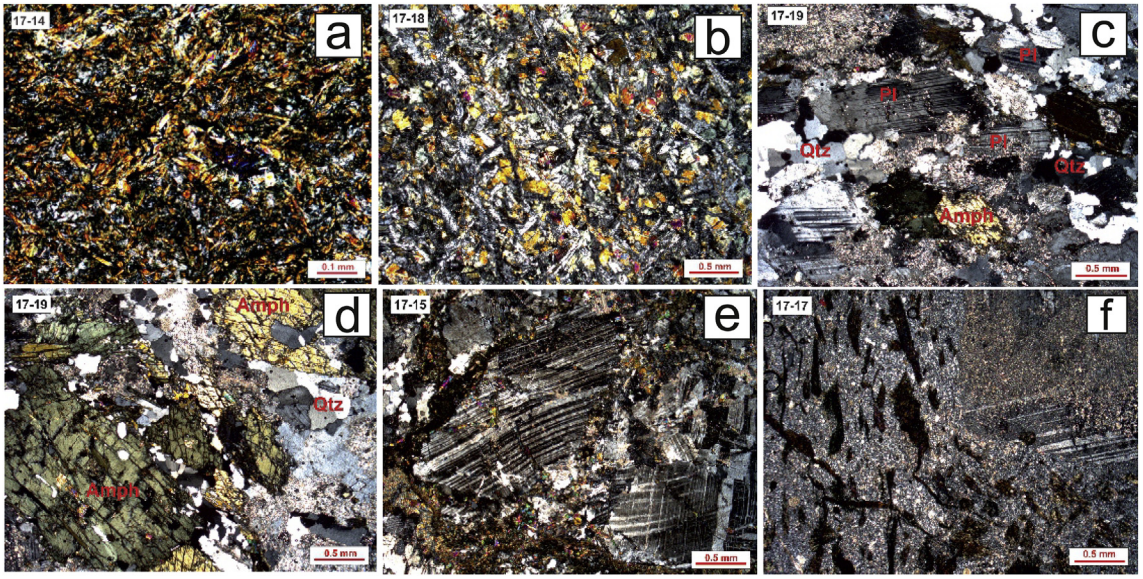

Fig. 4. Photomicrographs of thin sections from rocks of Lake Songkul area: (a) basalt from the north shore of Lake Songkul (sample 17-14), (b) basalt from the west shore of Lake Songkul (sample 17-18), (c) typical quartz diorite, (d) amphibole rich cluster in quartz diorite, (e) kinked plagioclase crystals in deformed quartz diorite, (f) diorite porphyry from endocontact zone. Cross polarized light. Abbreviations: Amph – amphibole, Pl – plagioclase, and Qtz – quartz.

Table 2
Chemical compositions of magmatic rocks from Lake Songkul area (major in wt.%, minor and trace in ppm).

Intrusion	Karakatty Fm. basalts							Songkul quartz diorites					
Rock-type													
Sample	17-14	17-18	17-16	17-19	AI-102	AI-99	AI-104	17-15	T5-068	AI-101	17-17	T5-070	AI-97
SiO_2	49.76	49.79	50.78	58.91	59.42	59.52	59.96	60.65	60.88	61.02	61.56	61.99	64.90
TiO_2	1.93	1.67	1.08	0.49	0.59	0.19	0.28	0.46	0.44	0.47	0.39	0.43	0.27
Al_2O_3	13.37	13.17	12.69	16.67	15.19	22.69	20.61	15.26	17.84	18.92	15.30	17.19	18.53
$Fe_2O_3^t$	14.90	14.16	11.11	6.33	6.98	2.17	3.24	5.87	4.85	5.43	4.91	4.74	2.81
MnO	0.24	0.19	0.19	0.12	0.11	0.04	0.06	0.10	0.100	0.07	0.07	0.098	0.07
MgO	5.66	6.61	11.18	3.13	4.15	0.98	1.31	2.95	1.75	1.32	2.77	1.77	0.63
CaO	8.07	7.75	5.44	6.53	5.02	4.45	5.05	5.43	6.46	5.97	4.39	5.76	2.37
Na_2O	2.32	3.69	2.73	3.68	4.94	6.28	6.08	4.68	3.70	4.57	5.42	3.87	6.86
K_2O	0.07	0.19	0.56	0.62	0.64	1.63	1.17	0.25	0.33	0.26	0.75	0.41	1.09
P_2O_5	0.21	0.19	0.22	0.13	0.10	0.06	0.07	0.11	0.17	0.11	0.16	0.15	0.05
LOI	2.75	1.97	3.19	2.60	2.41	1.34	1.52	3.58	1.10	1.25	3.35	1.57	1.51
SUM	99.25	99.37	99.17	99.22	99.55	99.35	99.35	99.35	97.61	99.38	99.06	97.96	99.07
Cr	107	153	1284	58	229	<100	<100	<100	14	<100	81	12	<100
Ni	<100	<100	138	<100	<100	<100	<100	<100	11	<100	<100	8	<100
V	585	531	353	241	268	79	119	230	88	150	165	90	77
Rb	1.03	2.3	8.9	10.0	18.3	33	5.1	5.4	4.6	2.6	13.0	6.8	26
Ba	56	87	215	422	584	774	443	247	197	173	266	312	298
Sr	356	218	122	662	743	1290	393	600	904	1025	568	878	908
Zr	143	122	147	54	33	40	67	52	77	62	71	75	39
Hf	3.11	3.20	3.69	1.49	0.90	0.93	1.82	1.37	1.24	1.78	1.95	1.08	0.98
Y	45.4	38.4	28.3	11.9	7.0	2.9	12.2	13.4	7.5	7.6	8.8	7.5	4.7
Nb	6.64	5.02	11.88	2.35	1.32	0.79	1.65	2.62	2.10	2.04	3.77	1.40	1.07
Ta	0.37	0.32	0.72	0.14	0.08	0.05	0.11	0.11	0.10	0.13	0.20	<0.1	0.05
U	0.23	0.17	1.48	0.41	0.24	0.27	0.69	0.35	0.34	0.21	1.10	0.26	0.12
Th	0.45	0.51	7.80	6.41	0.42	0.75	0.86	0.98	4.50	0.48	3.62	1.01	0.39
La	6.8	6.4	22.2	17.6	7.2	5.6	4.9	7.3	8.5	6.6	9.6	10.6	5.1
Ce	18.3	17.2	46.7	32.7	13.2	8.3	10.2	15.7	18.2	14.8	20.5	22.8	9.2
Pr	2.85	2.66	5.96	3.11	1.64	1.08	1.48	2.09	2.60	2.26	2.57	2.96	1.21
Nd	15.1	14.0	24.1	11.0	6.0	4.7	6.2	8.7	10.5	10.2	10.7	12.4	5.3
Sm	4.72	4.37	5.57	2.27	1.48	0.86	1.71	2.18	2.62	2.63	2.18	2.71	1.25
Eu	1.55	1.31	1.28	0.65	0.49	0.37	0.53	0.70	0.75	0.86	0.67	0.79	0.45
Gd	6.27	5.37	5.30	2.21	1.42	0.71	1.98	2.26	1.95	2.16	1.80	2.62	1.06
Tb	1.05	0.97	0.85	0.30	0.20	0.09	0.33	0.36	0.27	0.26	0.25	0.33	0.15
Dy	6.64	6.46	4.95	2.03	1.16	0.45	2.04	2.12	1.38	1.45	1.43	1.48	0.74
Ho	1.50	1.41	1.01	0.45	0.24	0.09	0.42	0.43	0.25	0.26	0.32	0.24	0.15
Er	4.32	3.94	2.77	1.27	0.71	0.28	1.30	1.33	0.74	0.70	0.89	0.77	0.44
Tm	0.65	0.56	0.39	0.19	0.11	0.05	0.20	0.20	0.11	0.11	0.14	0.14	0.07
Yb	3.94	3.67	2.50	1.22	0.72	0.33	1.23	1.28	0.81	0.75	0.92	0.77	0.45
Lu	0.60	0.55	0.37	0.18	0.11	0.05	0.19	0.20	<0.1	0.11	0.14	0.11	0.07
Mg#	42.93	48.04	66.58	49.47	54.07	47.23	44.40	49.86	41.62	32.43	52.78	41.38	30.81
Sr/Y	8	6	4	56	106	447	32	45	121	136	65	117	194
La/Yb	1.7	1.8	8.9	14.5	10.1	16.9	4.0	5.7	10.5	8.8	10.4	13.8	11.3

<100 – below detection limit.
$Fe_2O_3^t$–total Fe as Fe_2O_3.

also reflected in high LOI values in the range of 1–3.5 wt.% (Table 2). Rarely preserved fresh amphibole forms large clusters rich in accessory minerals (Fig. 4d). Major and trace elements were analyzed in 10 samples of Songkultau granitoids. The analyzed samples have SiO_2 contents in the range of 59–65 wt.% (Table 2). On the TAS classification diagram, compositions of the granitoids plot in the fields of diorite, granodiorite, monzonite and quartz monzonite (Fig. 5a). The rocks are characterized by metaluminous to slightly peraluminous compositions with ASI<1.1 (ASI = molar $Al_2O_3/(Na_2O + K_2O + CaO)$). They generally plot in the field of magnesian granites in the $FeO^t/(FeO^t + MgO)$ vs. SiO_2 diagram and in the field of Low-K series in the K_2O vs. SiO_2 diagram (Fig. 5b, d). In the ($Na_2O + K_2O$ – CaO) vs. SiO_2 diagram (Fig. 5c) compositions of the Songkultau granitoids form a subvertical trend and plot in the fields of calcic and alkali-calcic series. The REE spectra for the Songkultau granitoids are characterized by moderate LREE-enrichments and strong depletion in HREE without Eu anomalies (Fig. 6a). The primitive mantle-normalized multicationic diagram patterns show moderate enrichments in LILE, strong positive anomalies for Sr and distinct depletions in HFSE with negative anomalies for Nb and Ta (Fig. 6b).

In their chemical compositions, the Songkultau granitoids show close similarities with adakites – a group of acid volcanic rocks, described from Adak Island in the Aleutian arc, in which major and trace element chemistry suggested an origin by melting of subducted basaltic crust (Defant and Drummond, 1990). The Songkultau granitoids fit well the main chemical characteristics of adakites (high Sr/Y and La/Yb ratios, high Na_2O, elevated Mg# and relatively high Ni and Cr contents) (Table 2, Fig. 7) as defined by Defant and Drummond (1990), Drummond and Defant (1990), Richards and Kerrich (2007), Castillo (2012). Although it has been shown that adakitic rocks may form in various tectonic settings and their compositions can vary significantly (Castillo, 2012), we cautiously define Songkultau granitoids as adakite-like series and discuss their genesis below in Section 4.

The Karakatty Fm. in the immediate vicinity of the Songkultau intrusion is represented by homogeneous massive and pillow basalts (Fig. 3a) with sub-ophitic texture formed by plagioclase and clinopyroxene and matrix mainly consisting of secondary and opaque minerals (Fig. 4a and b). For comparison, chemical compositions of the Karakatty basalts are shown on classification and discrimination diagrams (Fig. 5)

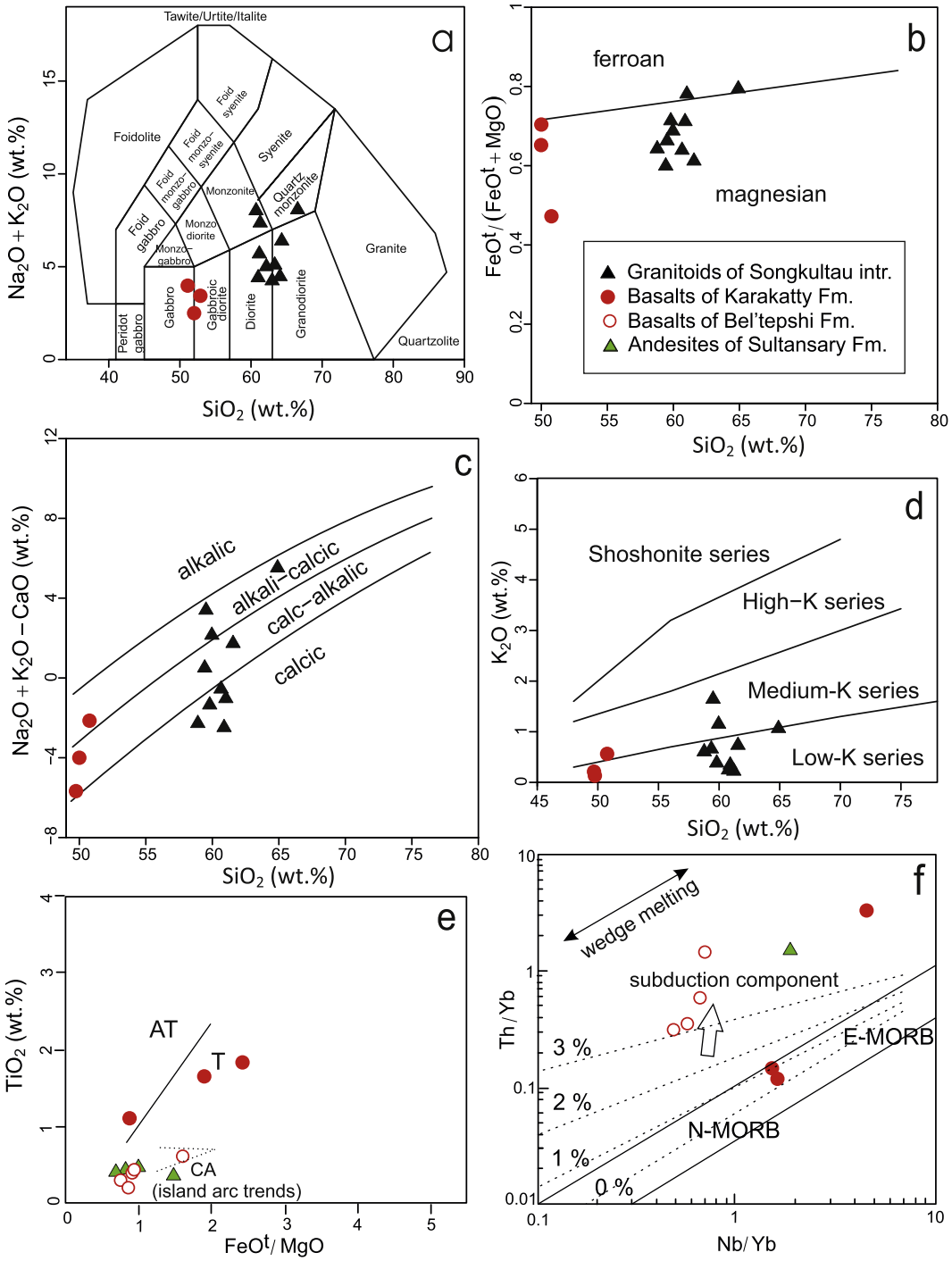

Fig. 5. Geochemical data for Songkultau granitoids and volcanics of the Karakatty, Bel'tepshi and Sultansary Fms. on classification and discrimination diagrams: (a) $Na_2O + K_2O$ vs. SiO_2 (TAS) diagram, fields after Middlemost (1994); (b) $FeO^t/(FeO^t + MgO)$ vs. SiO_2 diagram, fields after Frost and Frost (2008); (c) ($Na_2O + K_2O$–CaO) vs. SiO_2 diagram, fields after Frost and Frost (2008); (d) K_2O vs. SiO_2 diagram, fields after Le Maitre et al. (1989); (e) TiO_2 vs. FeO^t/MgO diagram, fields for abyssal tholeiite (AT), tholeiite (T) and calc-alkaline volcanic rocks (CA) are after Miyashiro (1973); (f) Nb/Yb vs. Th/Yb diagram from Pearce and Peate (1995), stippled lines show magma compositions comprising 0 to 3 wt.% of a subduction component (Pearce, 2008). Data for the Bel'tepshi and Sultansary Fms. from Alexeiev et al. (2019).

in combination with geochemical data on similar volcanics from the adjacent Bel'tepshi and Sultansary Fms. reported by Alexeiev et al. (2019). On the TAS classification diagram the Karakatty volcanics plot in the fields of basalt and basaltic andesite (Fig. 5a). On the FeO^t/MgO vs. TiO_2 diagram two less altered basalt samples (samples 17-14 and 17-18) are classified as oceanic tholeiites, while one strongly altered basalt sample plots in the field of arc tholeiites and is similar to basalts of the Bel'tepshi and Sultansary Fms. plotting along the trend of island arc volcanics (Fig. 5e). Concentrations of incompatible elements in the Karakatty basalts are generally within the range characteristic for the E-MORB rocks. However, they have elevated LREE contents in the range transitional between E-MORB and OIB type basalts. Compared to the Karakatty basalts, volcanics of the Bel'tepshi and Sultansary Fms. have lower concentrations of REE and LILE and show distinct negative Nb

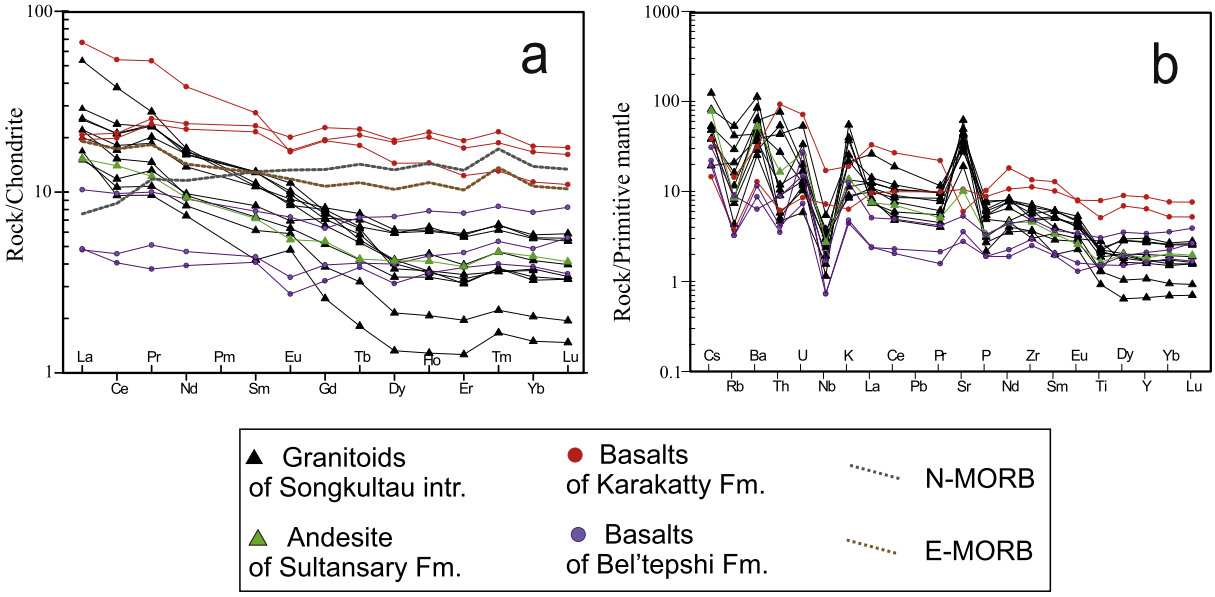

Fig. 6. Chondrite-normalized (Nakamura, 1974) REE patterns (a) and Primitive mantle-normalized (Sun and McDonough, 1989) trace element abundances (b) for magmatic rocks of Songkultau area. Andesite of Sultansary and basalts of Bel'tepshi Fms. are shown for comparison after Alexeiev et al. (2019).

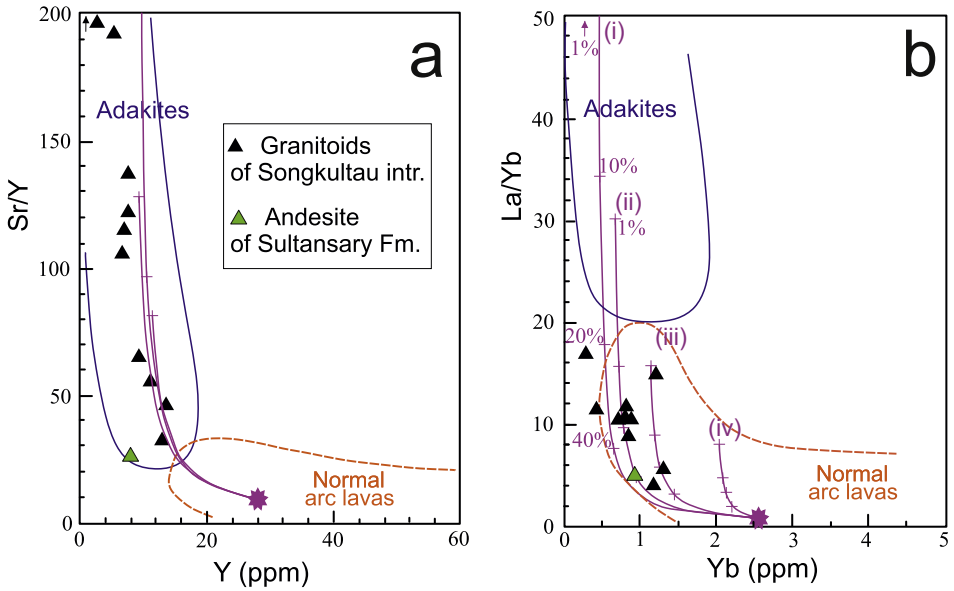

Fig. 7. Granitoids of Songkultau intrusion on discrimination diagrams (a) Sr/Y vs. Y and (b) La/Yb vs.Yb (after Drummond and Defant, 1990) that are used to distinguish adakite from normal arc andesite, dacite and rhyolite lavas. Field boundaries after Richards and Kerrich (2007). Solid curves represent partial melting trends after Castillo (2012) of (i) eclogite (50:50 pyroxene:garnet), (ii) 25% garnet amphibolite (25:75), (iii) 10% garnet amphibolite (10:90), and (iv) amphibolite, all with a starting normal-MORB bulk composition, shown by asterisk. Tick marks represent 1%, 10%, 20% and 40% partial melting of individual sources. Andesite of Sultansary Fm. is shown for comparison after Alexeiev et al. (2019).

anomaly on the primitive mantle-normalized multicationic diagram (Fig. 6). The suprasubduction origin of the Bel'tepshi and Sultansary volcanics is also illustrated by the Nb/Yb vs. Th/Yb diagram (Fig. 5f), where volcanics of the Bel'tepshi and Sultansary Fms. plot above the MORB-OIB array indicating a distinct sedimentary subduction component in these rocks, while the Karakatty basalts plot in the MORB-OIB array, which is characteristic for ocean floor basalts.

3.2. Zircon dating

Quartz diorite sample T5-070, chosen for SHRIMP U–Pb zircon chronology, supplied a homogeneous population of prismatic zircon grains with well-developed facets demonstrating simple oscillatory zoning and Th/U ratios in the range of 0.23–0.39, characteristic for magmatic zircon (Supplementary Table S3, Fig. 8). Ten spots were analyzed in seven grains. The U–Pb analytical data are presented in Supplementary Table S3 and on concordia diagram in Fig. 8. All ten analysis yielded concordant $^{206}Pb/^{238}U$ ages in the range of 526–494 Ma, for which a concordia age of 505.7 ± 5.3 Ma (MSWD = 0.11) was calculated. This age, interpreted as the crystallization age of the quartz diorite sample T5-070, coincides within error limits with the 502.7 ± 9.2 Ma and 498.3 ± 5.8 Ma LA-ICP-MS zircon ages, reported for the Songkultau granitoids by De Grave et al. (2011). Collectively, these ages define the emplacement age of the Songkultau intrusion to the middle–late Cambrian.

Gravellite of the Muztor Fm. (sample 17-20) produced a distinct population of detrital zircon grains, from which 21 grains were analyzed by LA-ICP-MS in the Hong Kong University (see Supplementary Material S2 for details). The analyzed zircon grains yielded concordant $^{206}Pb/^{238}U$ ages in the range of 518–471 Ma (Supplementary Table S4). Four youngest grains with ages 478–471 Ma suggest a lower Ordovician maximum depositional age of the Muztor gravellite. On the probability

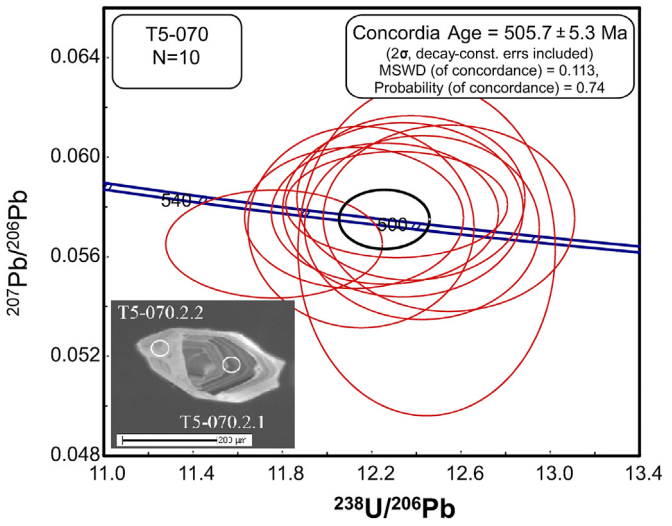

Fig. 8. Concordia diagram for zircon U–Pb SHRIMP data for quartz diorite of the Songkultau intrusion (sample T5-070).

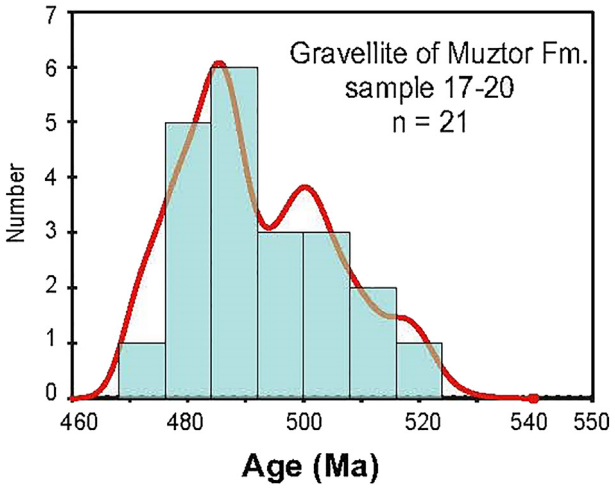

Fig. 9. Probability curve with histogram showing distribution of detrital zircon ages from gravellite of the Muztor Fm. (sample 17-20).

plot and histogram (Fig. 9), the ages form two peaks at ca. 485 Ma and 500 Ma. The smaller peak at ca. 500 Ma matches well with the age of the Songkultau intrusion while the major peak at ca. 485 Ma corresponds to the main phase of continental arc magmatism in the NTS (Konopelko et al., 2008; Alexeiev et al., 2019).

3.3. Nd isotopes and Hf-in-zircon analysis

We present the first Sm–Nd isotopic data for seven whole-rock samples of the Songkultau granitoids. Details of analytical procedures are given in Supplementary Material S2. Sm–Nd isotope data are listed in Supplementary Table S5 and shown in an isotope evolution diagram in Fig. 10. The initial isotopic ratios are calculated using the crystallization ages obtained in this study (Table 1) and the trace element concentrations reported in Table 2. All analyzed samples have positive $\varepsilon_{Nd}(t)$ values of +3.8 to +6.4 and Neoproterozoic Nd model ages T_{DM}* (0.89–0.71 Ga), indicating a major contribution from depleted sources, such as the mantle or juvenile crust. Quartz diorite sample T5-070 was additionally analyzed for its whole-rock Pb isotopic compositions and yielded initial Pb isotopic composition 18.1 for $^{206}Pb/^{204}Pb$, 15.7 for $^{207}Pb/^{204}Pb$ and 38.2 for $^{208}Pb/^{204}Pb$ (Supplementary Table S6).

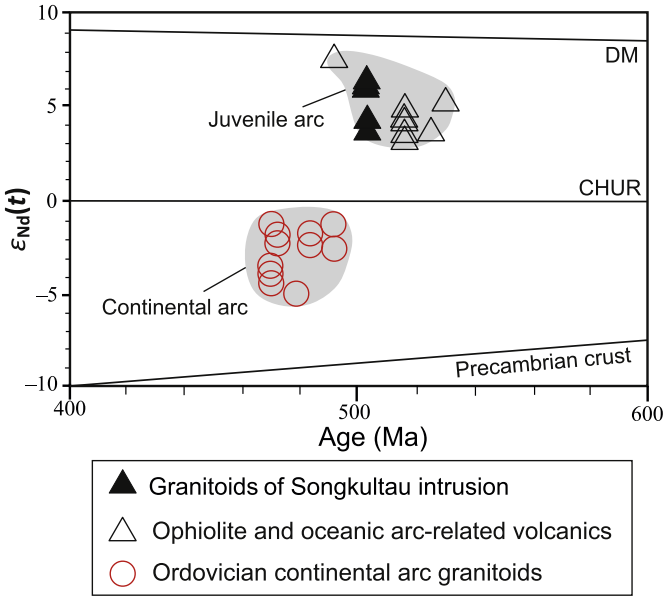

Fig. 10. Nd isotope evolution diagram for whole-rock samples of Songkultau granitoids. CHUR – chondritic uniform reservoir (after Jacobsen and Wasserburg, 1984). DM – depleted mantle (after Goldstein and Jacobsen, 1988). Published data for Cambrian ophiolite and primitive arc-related magmatic rocks and for Ordovician continental arc granitoids from adjacent areas of Kyrgyz Northern Tien Shan and Chinese Central Tien Shan are shown for comparison (data from Gao et al., 2009; Qian et al., 2009; Kröner et al., 2014; Alexeiev et al., 2019).

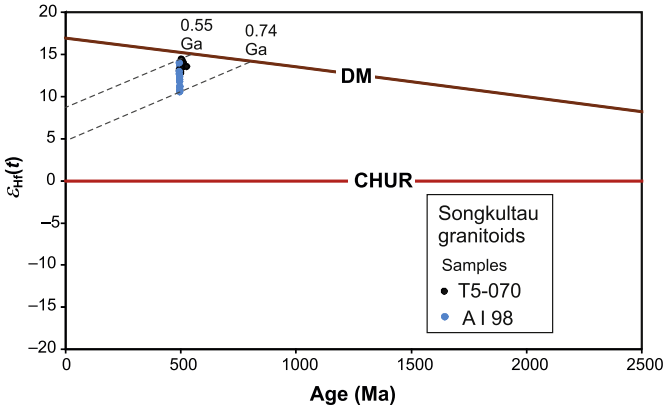

Fig. 11. Hf-in-zircon isotope evolution diagram for Songkultau granitoids. Solid line represents the depleted mantle evolution after Griffin et al. (2000). Minimum and maximum crustal model ages for the analyzed zircon grains from each sample are shown. Sample numbers as in Table 1.

Zircon domains from sample T5-070, dated by SHRIMP, and from sample AI-98, previously dated by De Grave et al. (2011), were also analyzed for their Lu–Hf isotopic compositions. The results, including $\varepsilon_{Hf}(t)$ and crustal model ages (t_{Hf}^{c}), are presented in Supplementary Table S7 and Fig. 11. Ten Lu–Hf isotopic spot analyses were performed on the same zircon domains that were analyzed for their Th–U–Pb isotopic compositions from sample T5-070 and all yielded similar initial $^{176}Hf/^{177}Hf$ ratios between 0.282819 and 0.282862, with corresponding $\varepsilon_{Hf}(t)$ values between +12.6 and +14.4 (mean +13.5) and crustal model ages (t_{Hf}^{c}) of 0.66–0.55 Ga (mean 0.62 Ga). Eleven Lu–Hf isotopic spot analyses were performed on the same zircon domains that were analyzed for their Th–U–Pb isotopic compositions from sample AI-98 (Supplementary Table S8). All eleven analyses yielded initial $^{176}Hf/^{177}Hf$ ratios between 0.282765 and 0.282850 corresponding to $\varepsilon_{Hf}(t)$ values between

+10.7 and +13.7 (mean +12.3) and crustal model ages (t_{Hf}^{c}) of 0.74 to 0.58 Ga (mean 0.65 Ga). The obtained Hf crustal model ages (t_{Hf}^{c}) in the range of 0.6–0.7 Ga are in good agreement with Nd model ages (T_{DM}*) in the range of 0.7–0.9 Ga (Table 1) and indicate derivation of the Songkultau granitoids from a juvenile source.

4. Discussion

4.1. Petrogenesis and magma sources of the Songkultau adakites

The Songkultau granitoids show close similarities with chemical characteristics of adakites (SiO_2 > 56 wt.%, Al_2O_3 > 15 wt.%, Na_2O > 3.5 wt.%, Na_2O > K_2O, elevated Mg# ~ 50 at 60 wt.% SiO_2, high Sr/Y > 40 and La/Yb > 20, relatively high Ni and Cr contents and Eu/Eu* ~ 1) as defined by Defant and Drummond (1990), Drummond and Defant (1990), Richards and Kerrich (2007), Castillo (2012). Previous studies have shown that magmatic rocks with adakitic geochemical signatures could originate from various tectono-magmatic processes, such as (i) melting of young and hot subducted oceanic slab, as it was originally proposed by Defant and Drummond (1990) and Martin et al. (2005); (ii) assimilation and fractional crystallization (AFC) or fractional crystallization (FC) processes (Macpherson et al., 2006); and (iii) melting of thickened lower crust or subducted continental crust (Chung et al., 2003).

The adakitic granitoids derived from partial melting of the mafic lower crust are usually potassium-rich (K_2O > Na_2O), and exhibit relatively fertile isotopic compositions with predominantly negative ε_{Nd} values and high Th/U, Th/Ba, and Rb/Ba ratios (Zheng et al., 2020 and references therein). These features are contrastingly different from the composition of slab-derived adakites, in general, and from the composition of the Songkultau granitoids, in particular. Therefore, the Songkultau adakites cannot have originated from partial melting of the mafic lower crust.

The origin of adakitic arc lavas by fractional crystallization of garnet and/or amphibole from basaltic magma within the garnet stability field was advocated by Macpherson et al. (2006). Adakites generated by this process usually exhibit variable and high Dy/Yb ratios (1.7–3.2) in addition to high La/Yb and Sr/Y ratios, and are often characterized by relatively fertile isotopic compositions (Macpherson et al., 2006; Richards and Kerrich, 2007). In contrast, the Songkultau adakites have distinctly juvenile Nd–Hf isotopic compositions and exhibit consistently low Dy/Yb ratios in the range of 1.4–1.9. In addition, arc volcanic series produced by fractional crystallization are expected to have almost identical Th/Zr ratios (Schiano et al., 2010). This is not the case for the Songkultau granitoids, where Th/Zr ratios vary significantly in the range of 0.01–0.12, which is more characteristic of a partial melting trend (Schiano et al., 2010). Finally, AFC and FC processes usually result in continuous compositional trends, which are also not the case for the Songkultau intrusion where mafic contemporaneous rocks are not known (Osmonbetov, 1982). On the other hand, although the compositional variations of the Songkultau adakites are relatively minor with SiO_2 concentrations in the range of 59–65 wt.% (Table 2), these variations can be explained by fractional crystallization as illustrated in the (Na_2O + K_2O–CaO) vs. SiO_2 diagram (Fig. 5c) where compositions of the Songkultau granitoids form a steep subvertical trend from calcic to alkali-calcic series, which is typical for magmatic suites formed by fractional crystallization of high-Ca mafic silicates, such as augite (Frost and Frost, 2008; Konopelko et al., 2011). Thus, it can be concluded that fractional crystallization, albeit responsible for minor compositional variations of the Songkultau adakites, probably was not the main process that controlled the genesis of this rock series.

Geological and geochemical features of the Songkultau granitoids are in good agreement with their origin by melting of subducted oceanic slab. The Songkultau intrusion is located within the Terskey Suture zone in association with ophiolites and volcanics with mixed ocean floor and island arc affinities indicating a primitive arc tectonic setting. As shown above, the compositions of the Songkultau granitoids match well the main chemical characteristics of the slab-derived adakites. The Songkultau rocks have concentrations of MgO in the range of 0.6–4.1 wt.% at silica contents of 58.9–64.9 wt.% (Table 2) and generally correspond to high-SiO_2 adakites indicating their affinity with adakites in the sense of Defant and Drummond (1990) who suggested an origin by melting of young subducted basaltic crust for these high-SiO_2 adakite types. The La/Yb ratios in the Songkultau granitoids are below 20 and do not fit the latest adakite definition of Richards and Kerrich (2007) (Fig. 7), however, they are in the range La/Yb > 5 proposed for adakites in the original work of Defant and Drummond (1990). Experimental studies in combination with geochemical evidence show that high-SiO_2 adakites can be derived by partial melting of depleted mafic to ultramafic sources. This is most likely to occur between the garnet-in and amphibole-out phase boundary, where the garnet is present as a residual phase between 0.7 GPa and 2.6 GPa at temperatures of 650–1050 °C for hydrous basaltic compositions (e.g. Defant and Drummond, 1990; Martin et al., 2005; Thorkelson and Breitsprecher, 2005; Castillo, 2012 and references therein). These melting conditions occur at convergent margins where young and, thus, still hot oceanic slabs are being subducted (Castillo, 2012). The geochemical characteristics of the Songkultau granitoids closely correspond to experimental melt compositions produced by 10%–20% partial melting of garnet amphibolite containing 10%–25% of garnet (Fig. 7). Experimental melts, produced by melting of eclogite and amphibolite, show Mg# around 44, while higher Mg#, characteristic for many adakites, can be explained by assimilation of peridotite from the overlying mantle wedge. Rapp et al. (1999) have shown that assimilating 10–16% peridotite tends to increase Mg# of the resulting melt from 44 to 56. Because several analyzed samples of the Songkultau granitoids, including those with lowest silica concentrations, have Mg# as high as 49–54, it can be suggested that limited interaction with peridotite of the mantle wedge took place during their formation. On the other hand, as noted above, the observed variation in Mg# can be explained by fractional crystallization, which is supported by general trend of decreasing Mg# with increasing silica contents (Table 2).

Consistently juvenile Nd–Hf isotopic compositions of the Songkultau granitoids (Table 1) are also in agreement with their origin by melting of subducted oceanic crust. The analyzed samples are characterized by positive $\varepsilon_{Nd}(t)$ (+3.8 to +6.4) and $\varepsilon_{Hf}(t)$ (+12.3 to +13.5) values, and by Neoproterozoic model ages (0.96–0.71 Ga) in combination with low initial $^{206}Pb/^{204}Pb$ (18.1), indicating a major contribution from long-term lithophile element depleted sources such as the mantle or juvenile crustal rocks with only a short residence time before magma genesis. In addition, all $\varepsilon_{Hf}(t)$ values from sample T5-070 are virtually identical and those from sample AI-98 fall within a narrow range, suggesting a very homogeneous protolith (Fig. 11). However, although the Songkultau granitoids are characterized by positive $\varepsilon_{Nd}(t)$ and $\varepsilon_{Hf}(t)$ values, indicating derivation from MORB-like sources, their Nd–Hf isotopic compositions are slightly enriched, compared to compositions derived by melting of normal MORB with $\varepsilon_{Nd}(t)$ > +10 and $\varepsilon_{Hf}(t)$ > +15. This deviation is characteristic for many Phanerozoic adakites and is usually explained by interaction with enriched material of a "continental" mantle wedge and/or at the base of the crust, and by contamination with melts produced from subducted sediments (Castillo, 2012 and references therein). The latter scenario is in agreement with slightly elevated K_2O contents (up to 1.6 wt.%) in the Songkultau adakites, because partial melting of subducted sediments associated with underlying oceanic crust may generate potassium-enriched melts, as shown in several experimental petrological studies (e.g. Hermann and Spandler, 2008). Input from subducted sediments is also registered in compositions of volcanic rocks spatially associated with the Songkultau intrusion in the Terskey Suture zone. This is illustrated by the Nb/Yb vs. Th/Yb diagram of Pearce et al. (1984) and Pearce and Peate (1995), utilizing Th as a proxy to estimate a sedimentary subduction component in basalts. On this diagram (Fig. 5f), volcanics of the Bel'tepshi and Sultansary Fms., which have juvenile isotopic compositions similar to Songkultau granitoids,

plot above the MORB-OIB array indicating a distinct minor sedimentary subduction component in these rocks. Thus, geological and geochemical characteristics of the Songkultau adakites convincingly support their origin by melting of young and hot subducted oceanic crust with possible minor input from subducted sediments and interaction with the overlying mantle wedge.

4.2. Implications for the early Paleozoic tectonic evolution of northern Tien Shan

The main phase of the voluminous Andean type magmatism in the NTS is relatively well constrained by ca. 490–475 Ma ages of suprasubduction granitoids, indicating that in the late Cambrian–early Ordovician a single continental magmatic arc occupying the whole NTS domain has been formed (Alexeiev et al., 2019). However, the early–middle Cambrian tectonic evolution of the NTS remains poorly studied due to scarcity of geochronological and geochemical data. In their latest review, Alexeiev et al. (2019) suggested that initiation of the continental arc magmatism in the NTS took place at ca. 510 Ma and was preceded by an older Neoproterozoic episode of intraplate magmatism and by formation of the early Cambrian intra-oceanic arc in the Terskey Ocean south of the NTS microcontinent. This hypothetical Sultansary intra-oceanic arc, which was defined by Mikolaichuk et al. (1997) based on their studies of Cambrian volcanic formations to the east of Lake Songkul, was, according to Alexeiev et al. (2019), accreted to the NTS in the late Cambrian at ca. 510–500 Ma.

In order to better understand the geotectonic setting of Cambrian volcanic formations from the Terskey Suture zone, chemical compositions of the Karakatty basalts, presented in this study, are discussed below in combination with published geochemical data on similar volcanics from adjacent Bel'tepshi and Sultansary Fms. Concentrations of incompatible elements in the Karakatty basalts are generally within the range characteristic for E-MORB rocks. However, they have elevated LREE and Nb contents that suggest a more transitional nature between E-MORB and OIB type basalts. Sample 17-16 contains 11 ppm Nb (Table 2) and can be defined as a high-Nb basalt (Nb $\geq$ 7 ppm) according to Castillo (2012). Elevated LREE and Nb contents distinguish the Karakatty basalts from volcanics of the Bel'tepshi and Sultansary Fms., which have lower concentrations of REE and LILE and show distinct negative Nb anomaly on the primitive mantle-normalized multicationic diagram (Fig. 6), indicating their similarity with subduction-related volcanic series. This is in accordance with the Nb/Yb vs. Th/Yb diagram of Pearce and Peate (1995), utilizing Th as a proxy to estimate a sedimentary subduction component in basalts (Fig. 5f), where two less altered samples of the Karakatty basalts (samples 17-14 and 17-18) plot in the MORB-OIB data array, while volcanics of the Bel'tepshi and Sultansary Fms. and one altered sample of the Karakatty basalt plot above the MORB-OIB array, indicating a distinct minor sedimentary subduction component in these rocks. Similar differences between the two groups of volcanics can be illustrated utilizing the FeO^t/MgO vs. TiO_2 diagram of Miyashiro (1973), where two less altered samples of the Karakatty basalts are classified as oceanic tholeiites while the Bel'tepshi and Sultansary volcanics plot along the trend of island arc series (Fig. 5e). Thus, chemical compositions of the Cambrian volcanics from the Terskey Suture zone vary from ocean floor tholeiites with transitional E-MORB – OIB affinities to typical suprasubduction volcanic series. This compositional variation can be interpreted as a result of tectonic juxtaposition of various arc and subducting plate sections during accretion.

Despite variations in chemical composition, all analyzed rocks from the Terskey Suture zone have consistently juvenile isotopic compositions. A transition from a primitive to mature continental arc development can be traced utilizing published isotopic data from adjacent areas of the Kyrgyz Northern Tien Shan and Chinese Central Tien Shan domains. This is illustrated in Figs. 10 and 12, where formations of a juvenile arc are characterized by strongly positive $\varepsilon_{Nd}(t)$ and $\varepsilon_{Hf}(t)$ values while younger continental arc granitoids have mixed and negative $\varepsilon_{Nd}(t)$ and $\varepsilon_{Hf}(t)$ values. This trend may rather reflect a spatial than temporal distribution of juvenile and crustal magmatic rocks because in the NTS there exist several magmatic series with U–Pb zircon ages in the range of 525–500 Ma, where isotopic compositions were not analyzed (Konopelko et al., 2012, 2014; Alexeiev et al., 2019). However, available Nd–Hf isotopic data, presented in Figs. 10 and 12, show that juvenile magmatic series, associated with the Terskey Suture zone bound to the southern margin of the NTS, are slightly older (generally > 495 Ma) than granitoids with crustal and mixed signatures, which were emplaced inside the NTS domain during the main phase of the Andean-type continental arc magmatism (generally < 495 Ma).

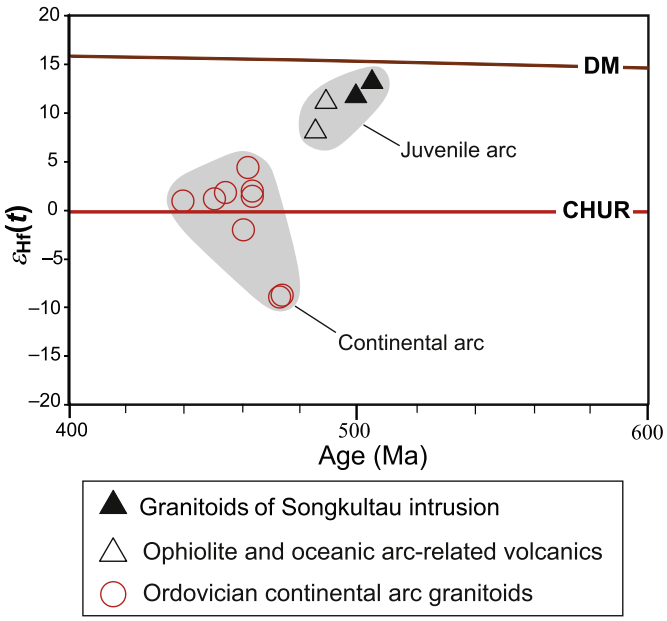

Fig. 12. Hf-in-zircon isotope evolution diagram for Cambrian ophiolite and primitive arc-related magmatic rocks and for Ordovician continental arc granitoids from the Kyrgyz Northern Tien Shan and Chinese Central Tien Shan. Symbols represent mean $\varepsilon_{Hf}(t)$ values for each sample. Data from Huang et al. (2013), Ma et al. (2013), Kröner et al. (2014), Rojas-Agramonte et al. (2014), Alexeiev et al. (2019) and this study.

Alexeiev et al. (2019) suggested that early Cambrian formations of the Terskey Suture zone formed in the Terskey Ocean south of the NTS microcontinent and in the Sultansary intra-oceanic arc that was accreted to the NTS in the middle Cambrian at ca. 510 Ma. We collectively define these primitive island arc and ocean floor rock assemblages as the juvenile Cambrian arc of the NTS, emphasizing that, combined with the large Songkultau intrusion (ca. 70 km^2), they constitute a significant in size juvenile block located in predominantly crustal terranes of Kyrgyz Tien Shan. Adakitic affinity and juvenile isotopic compositions of the ca. 500 Ma old Songkultau granitoids may indicate that hot subduction in this arc continued until middle-late Cambrian. Obduction of the juvenile arc complexes onto the NTS prior to the main phase of the continental arc magmatism could be explained by transition from slab retreating to slab advancing environment (e.g. Cawood et al., 2009). This accretionary episode is also documented by HP-UHP metamorphism, followed by the rapid uplift of the NTS and the formation of coarse clastic sediments in the intermontane basins. A lower Ordovician depositional age of ca. 478–471 Ma, obtained for the gravellite of the Muztor Fm., is in agreement with ages of lower–middle Ordovician coarse clastic sediments elsewhere in the Northern Tien Shan (Mikolaichuk et al., 1997). In particular, similar depositional age of ca. 470–465 Ma was reported for conglomerates about 50 km east of Songkultau by Konopelko et al. (2008) based on single grain U–Pb zircon dating of granite pebbles. The distribution of ages of detrital zircon grains from the Muztor gravellite

shows a smaller peak at ca. 500 Ma, which matches well the age of the Songkultau intrusion and suggests derivation of the Muztor conglomerates from a proximal source (Fig. 9). The major peak at ca. 485 Ma corresponds to the main phase of the Andean-type subduction-related magmatism in the NTS that was associated with rapid uplift and erosion.

Thus, the here investigated magmatic suites of the Terskey Suture zone are interpreted as a relic of a primitive Cambrian arc comprising substantial in size juvenile block that has been identified so far in the predominantly crustal domains of the Tien Shan orogenic belt. On a regional scale, this primitive arc can be compared with juvenile Cambrian arcs of Chinese Tien Shan (Gao et al., 2009; Ma et al., 2013; Wang et al., 2015), Kazakhstan (Ryazantsev et al., 2009; Degtyarev, 2012; Liu et al., 2016), Gorny Altai (Buslov et al., 2002) and the Lake Zone of Mongolia (Janoušek et al., 2018) that formed as a result of the onset of convergence between the Palaeo-Asian oceanic plate and the surrounding continents after break-up of the Rodinia supercontinent (Domeier and Torsvik, 2014).

5. Conclusions

The Songkultau intrusion is spatially associated with the Terskey Suture zone bound to the southern margin of the Northern Tien Shan domain. The intrusion is composed of coarse-grained gneissose quartz diorites and tonalities, which fit the main chemical characteristics of the high-SiO_2 adakites ($SiO_2 > 56$ wt.%, $Al_2O_3 > 15$ wt.%, $Na_2O > 3.5$ wt.% and high Sr/Y and La/Yb ratios) and are classified as granitoids with adakite geochemical affinities. The Songkultau granitoids have positive initial ε_{Nd} (+3.8 to +6.4) and ε_{Hf} (+12.3 to +13.5) values indicating that they were derived from sources with MORB-like isotopic signature. The granitoids are spatially associated with pillow basalts with mixed ocean floor and island arc geochemistry. This rock assemblage is interpreted as a relic of an early-middle Cambrian juvenile arc where the adakite-like granitoids were produced by partial melting of young and, thus, still hot subducted oceanic crust. An age of ca. 505 Ma, obtained for the Songkultau intrusion, shows that hot subduction under the NTS continued until middle Cambrian. The primitive arc formations were obducted onto the NTS domain, where the Andean type continental magmatic arc developed in Cambrian and Ordovician. Formation of the Andean type arc was accompanied by rapid uplift and erosion. This process was documented by deposition of coarse clastic sediments represented in the Lake Songkul area by the conglomerates of the Muztor Fm. A lower Ordovician depositional age of ca. 478–471 Ma, obtained for the gravellite of the Muztor Fm., is in agreement with ages of conglomerates elsewhere in the Northern Tien Shan. The presence of ca. 500 Ma detrital zircon grains in the Muztor gravellite, which are similar in age to the Songkultau granitoids, suggests that the sediments were derived from proximal sources. Collectively, the Songkultau adakites and associated ocean floor and island arc formations of the Terskey Suture zone constitute a relic of a juvenile Cambrian arc and represent a juvenile domain of substantial size identified so far within the predominantly crustal terranes of the Tien Shan orogenic belt.

Declaration of competing interest

The authors declare that they have no known competing financial interests or personal relationships that could have appeared to influence the work reported in this paper.

Acknowledgements

We are grateful to Anatoly Ilyukhin, Gilby Jepson, Jack Gillespie and Alina Perfilova who were involved in field work and sample preparation. Insightful comments of Tao Wang, Dmitry Alexeiev and an anonymous reviewer helped to improve the manuscript significantly. Dmitry Alexeiev is also acknowledged for his generous support during the first field campaign at Songkultau. The study was supported by the Ministry of Education and Science of the Russian Federation (Project No 14.Y26.31.0018 – I.S., D.K.). D. Konopelko acknowledges C0LLAB travel grant from SPbGU and support through the Natural History Museum, London where part of the study was carried out in the frame of Research Fellowships at the Centre for Russian and Central EurAsian Mineral Studies (CERCAMS). RS acknowledges funding under Natural Environment Research Council Grant NE/P017452/1 “From arc magmas to ores (FAMOS): A mineral systems approach”. This is a contribution to the State Assignment of the Sobolev Institute of Geology and Mineralogy SB RAS (I.S.) and IGCP 662 Project “Orogenic Architecture and Crustal Growth from Accretion to Collision” under the patronage of UNESCO-IUGS.

Appendix A. Supplementary data

Supplementary data to this article can be found online at https://doi.org/10.1016/j.gsf.2020.08.006.

References

Alexeiev, D.V., Kröner, A., Hegner, E., Rojas-Agramonte, Y., Biske, Y.S., Wong, J., Geng, H.Y., Ivleva, E.A., Mühlberg, M., Mikolaichuk, A.V., Liu, D., 2016. Middle to Late Ordovician arc system in the Kyrgyz Middle Tianshan: from arc–continent collision to subsequent evolution of a Palaeozoic continental margin. Gondwana Res. 39, 261–291.

Alexeiev, D.V., Bykadorov, V.A., Volozh, YuA., Sapozhnikov, R.B., 2017. Kinematic analysis of Jurassic grabens of southern Turgai and the role of the Mesozoic stage in the evolution of the Karatau–Talas–Ferghana strike-slip fault, southern Kazakhstan and Tian Shan. Geotectonics 51 (2), 105–120.

Alexeiev, D.V., Kröner, A., Kovach, V.P., Tretyakov, A.A., Rojas-Agramonte, Ya, Degtyarev, K.E., Mikolaichuk, A.V., Wong, J., Kiselev, V.V., 2019. Evolution of cambrian and early Ordovician arcs in the Kyrgyz North Tianshan: insights from U-Pb zircon ages and geochemical data. Gondwana Res. 66, 93–115.

Bakirov, A.B., Maksumova, R.A., 2001. Geodynamic evolution of the Tien Shan lithosphere. Russ. Geol. Geophys. 42, 1359–1366.

Biske, Yu.S., Seltmann, R., 2010. Paleozoic Tian-Shan as a transitional region between the Rheic and Urals-Turkestan oceans. Gondwana Res. 17, 602–613.

Burtman, V.S., 2010. Tien Shan, Pamir, and Tibet: history and geodynamics of Phanerozoic oceanic basins. Geotectonics 44 (5), 388–404.

Burtman, V.S., 2015. Tectonics and geodynamics of the Tian Shan in the middle and late Paleozoic. Geotectonics 49 (4), 302–319.

Buslov, M.M., Watanabe, T., Saphonova, I.Yu, Iwata, K., Travin, A., Akiyama, M., 2002. Vendian-cambrian island arc system of the siberian continent in Gorny Altai (Russia, Central Asia). Gondwana Res. 5 (4), 781–800.

Castillo, P.R., 2012. Adakite petrogenesis. Lithos 134–135, 304–316.

Cawood, P.A., Kröner, A., Collins, W.J., Kusky, T.M., Mooney, W.D., Windley, B.F., 2009. Accretionary orogens through Earth history. Geological Society, London, Special Publications 318, 1–36.

Chung, S.L., Liu, D., Ji, J., Chu, M.F., Lee, H.Y., Wen, D.J., Lo, C.H., Lee, T.Y., Qian, Q., Zhang, Q., 2003. Adakites from continental collision zones: melting of thickened lower crust beneath southern Tibet. Geology 31, 1021–1024.

Defant, M.J., Drummond, M.S., 1990. Derivation of some modern arc magmas by melting of young subducted lithosphere. Nature 347, 662–665.

De Grave, J., Glorie, S., Buslov, M.M., Izmer, A., Fournier-Carrie, A., Batalev, V., Vanhaecke, F., Elburg, M., Van den haute, P., 2011. The thermo-tectonic history of the Song-Kul Plateau, Kyrgyz Tien Shan: constraints by apatite and titanite thermochronometry and zircon U/Pb dating. Gondwana Res. 20 (4), 745–763.

Degtyarev, K.E., 2012. Tectonic Evolution of the Early Paleozoic Island Arcs and Continental Crust Formation in Caledonides of Kazakhstan. Transactions 602. GEOS. Geological Institute RAS, Moscow, p. 289 (in Russian).

Degtyarev, K.E., Ryazantsev, A.V., Tretyakov, A.A., Tolmacheva, T.Yu, Yakubchuk, A.S., Kotov, A.B., Salnikova, E.B., Kovach, V.P., 2013. Neoproterozoic–early Paleozoic tectonic evolution of the western part of the Kyrgyz ridge (Northern Tian Shan) Caledonides. Geotectonics 47, 377–417.

Demina, L.I., Lomize, M.G., Avdonin, A.V., 1995. Geodynamic Characteristics of Peridotites from Songkel Area (Northern Tianshan). Series 4 – Geology, vol. 1. “Vestnik” of Moscow State University, pp. 91–99 (in Russian).

Domeier, M., Torsvik, T.H., 2014. Plate tectonics in the late Paleozoic. Geosci. Front. 5, 303–350.

Drummond, M.S., Defant, M.J., 1990. A model for trondhjemite–tonalite–dacite genesis and crustal growth via slab melting: archaean to modern comparisons. J. Geophys. Res. 95, 21503–21521.

Dzhenchuraeva, A.V., Zacharov, I.L., Zhukov, J.V., Getman, O.F., Maksumova, R.A., Neevin, A.V., Nogaeva, L.P., Rinenberg, R.E., 2015. Stratified Rocks of Kyrgyzstan. Bishkek, p. 338 (in Russian).

Frost, B.R., Frost, C.D., 2008. A geochemical classification for feldspathic igneous rocks. J. Petrol. 49, 1955–1969.

Gao, J., Long, L.L., Klemd, R., Qian, Q., Liu, D.N., Xiong, X.M., Su, W., Liu, W., Wang, Y.T., Yang, E.Q., 2009. Tectonic evolution of the South Tianshan orogen and adjacent

regions, NW China: geochemical and age constraints of granitoid rocks. Int. J. Earth Sci. 98, 1221–1238.
Ghes, M.D., 2008. Terrane Structure and Geodynamic Evolution of the Caledonides of Tian-Shan. Altyn Tamga Publishing House, Bishkek, p. 158 (in Russian).
Goldstein, S.J., Jacobsen, S.B., 1988. Nd and Sr isotopic systematics of river water suspended material: implications for crustal evolution. Earth Planet Sci. Lett. 87, 249–265.
Griffin, W.L., Pearson, N.J., Belousova, E., Jackson, S.E., van Achterbergh, E., O'Reilly, S.Y., Shee, S.R., 2000. The Hf isotope composition of cratonic mantle: LAM-MC-ICPMS analysis of zircon megacrysts in kimberlites. Geochem. Cosmochim. Acta 64, 133–147.
Hermann, J., Spandler, C.J., 2008. Sediment melts at sub-arc depths: an experimental study. J. Petrol. 49 (4), 717–740.
Huang, Z.Y., Long, X.P., Kröner, A., Yuan, C., Wang, Q., Sun, M., Zhao, G.C., Wang, Y.J., 2013. Geochemistry, zircon U-Pb ages and Lu-Hf isotopes of early Paleozoic plutons in the northwestern Chinese Tianshan: petrogenesis and geological implications. Lithos 182–183, 48–66.
Jacobsen, S.B., Wasserburg, G.J., 1984. Sm–Nd evolution of chondrites and achondrites, II. Earth Planet Sci. Lett. 67, 137–150.
Jahn, B.M., 2004. The Central Asian orogenic belt and growth of the continental crust in the Phanerozoic. Geological Society, London, Special Publications 226, 73–100.
Jahn, B.-M., Wu, F., Chen, B., 2000. Massive granitoid generation in Central Asia: Nd isotope evidence and implication for continental growth in the Phanerozoic. Episodes 23 (2), 82–92.
Janoušek, V., Jiang, Y., Buriánek, D., Schulmann, K., Hanžl, P., Soejono, I., Kröner, A., Altanbaatar, B., Erban, V., Lexa, O., Ganchuluun, T., Košler, J., 2018. Cambrian–Ordovician magmatism of the Ikh-Mongol arc system exemplified by the Khantaishir magmatic complex (Lake Zone, south–central Mongolia). Gondwana Res. 54, 122–149.
Jepson, G., Glorie, S., Konopelko, D., Gillespie, J., Danišík, M., Evans, N.J., Mamadjanov, Y., Collins, A.S., 2018. Thermochronological insights into the structural contact between the Tian Shan and Pamirs, Tajikistan. Terra Nova 30, 95–104.
Kiselev, V.V., 1999. U−Pb Zircon Geochronology of Magmatic Rocks of the Northern Tien Shan. "Izvestiya" National Academy of Sciences of Kyrgyzstan, pp. 21–33 (in Russian).
Kiselev, V.V., Maksumova, R.A., 2001. Geology of the Northern and Middle Tien Shan: principal outlines. In: Seltmann, R., Jenchuraeva, R. (Eds.), Paleozoic Geodynamics and Gold Deposits in the Kyrgyz Tien Shan. IAGOD Guidebook Series 9. Natural History Museum, London, pp. 21–28.
Konopelko, D., Klemd, R., 2016. Deciphering protoliths of the (U)HP rocks in the Makbal metamorphic complex, Kyrgyzstan: geochemistry and SHRIMP zircon geochronology. Eur. J. Mineral 28 (6), 1233–1253.
Konopelko, D., Biske, G., Seltmann, R., Kiseleva, M., Matukov, D., Sergeev, S., 2008. Deciphering Caledonian events: timing and geochemistry of the Caledonian magmatic arc in the Kyrgyz Tien Shan. J. Asian Earth Sci. 32, 131–141.
Konopelko, D., Biske, G., Kullerud, K., Seltmann, R., Divaev, F., 2011. The Koshrabad granite massif in Uzbekistan: petrogenesis, metallogeny and geodynamic setting. Russ. Geol. Geophys. 52 (12), 1563–1573.
Konopelko, D., Klemd, R., Petrov, S.V., Apayarov, F., Nazaraliev, B., Vokueva, O., Scherstén, A., Sergeev, S., 2017. Precambrian gold mineralization at Djamgyr in the Kyrgyz Tien Shan: tectonic and metallogenic implications. Ore Geol. Rev. 86, 537–547. https://doi.org/10.1016/j.oreeorev.2017.03.007.
Konopelko, D., Kullerud, K., Apayarov, F., Sakiev, K., Baruleva, O., Ravna, E., Lepekhina, E., 2012. SHRIMP zircon chronology of HP-UHP rocks of the Makbal metamorphic complex in the Northern Tien Shan, Kyrgyzstan. Gondwana Res. 22, 300–309.
Konopelko, D., Biske, G., Seltmann, R., Petrov, S.V., Lepekhina, E., 2014. Age and petrogenesis of the Neoproterozoic Chon-Ashu alkaline complex, and a new discovery of chalcopyrite mineralization in the eastern Kyrgyz Tien Shan. Ore Geol. Rev. 61, 175–191.
Konopelko, D., Biske, YuS., Kullerud, K., Ganiev, I., Seltmann, R., Brownscombe, W., Mirkamalov, R., Wang, B., Safonova, I., Kotler, P., Shatov, V., Sun, M., Wong, J., 2019. Early Carboniferous metamorphism of the Neoproterozoic South Tien Shan-Karakum basement: new geochronological results from Baisun and Kyzylkum, Uzbekistan. J. Asian Earth Sci. 177, 275–286.
Kröner, A., Alexeiev, D.V., Rojas-Agramonte, Y., Hegner, E., Wong, J., Xia, X., Belousova, E., Mikolaichuk, A.V., Seltmann, R., Liu, D.Y., Kiselev, V.V., 2013. Mesoproterozoic (Grenville-age) terranes in the Kyrgyz North Tianshan: zircon ages and Nd-Hf isotopic constraints on the origin and evolution of basement blocks in the southern Central Asian Orogen. Gondwana Res. 23, 272–295.
Kröner, A., Kovach, V., Belousova, E., Hegner, E., Armstrong, R., Dolgopolova, A., Seltmann, R., Alexeiev, D.V., Hoffmann, J.E., Wong, J., Sun, M., Cai, K., Wang, T., Tong, Y., Wilde, S.A., Degtyarev, K.E., Rytsk, E., 2014. Reassessment of continental growth during the accretionary history of the Central Asian orogenic belt. Gondwana Res. 25, 103–125.
Kröner, A., Kovach, V., Alexeiev, D., Wang, K.-L., Wong, J., Degtyarev, K., Kozakov, I., 2017. No excessive crustal growth in the Central Asian Orogenic Belt: further evidence from field relationships and isotopic data. Gondwana Res. 50, 135–166.
Le Maitre, R.W., Bateman, P., Dudek, A., Keller, J., Lameyre, J., Le Bas, M.J., Sabine, P.A., Schmid, R., Sorensen, H., Streckeisen, A., Woolley, A.R., Zanettin, B., 1989. A Classification of Igneous Rocks and Glossary of Terms. Blackwell, Oxford.
Lomize, M.G., Demina, L.I., Zarshchikov, A.A., 1997. The Kyrgyz-Terskei paleoceanic basin, Tien Shan. Geotectonics 31, 463–482.
Liu, B., Han, B.F., Xu, Z., Ren, R., Zhang, J.R., Zhou, J., Su, Li, Li, Q.L., 2016. The Cambrian initiation of intra-oceanic subduction in the southern Paleo-Asian Ocean: further evidence from the Barleik subduction related metamorphic complex in the West Junggar region, NW China. J. Asian Earth Sci. 123, 1–21.
Ma, X.X., Shu, L.S., Santosh, M., Li, J.Y., 2013. Petrogenesis and tectonic significance of an early Palaeozoic mafic-intermediate suite of rocks from the Central Tianshan, northwest China. Int. Geol. Rev. 55, 548–573.
Macpherson, C.G., Dreher, S.T., Thirlwall, M.F., 2006. Adakites without slab melting: high pressure differentiation of island arc magma, Mindanao, the Philippines. Earth Planet Sci. Lett. 243, 581–593.
Maksumova, R.A., Zakharov, I.L., Zima, M.B., Khristova, M.P., Chernyshuk, V.P., 1988. Imbricated Overthrust Structure of the Early Caledonides of the Tien-Shan with New Data on Stratigraphy of the Lower Palaeozoic Deposits. Precambrian and Lower Palaeozoic of the Tien-Shan. Ilim Publishing House, Frunze, pp. 144–156 (in Russian).
Martin, H., Smithies, R.H., Rapp, R., Moyen, J.F., Champion, D., 2005. An overview of adakite, tonalite–trondhjemite–granodiorite (TTG), and sanukitoid: relationships and some implications for crustal evolution. Lithos 79, 1–24.
Middlemost, E.A.K., 1994. Naming materials in the magma/igneous rock system. Earth Sci. Rev. 37, 215–224.
Mikolaichuk, A.V., Kurenkov, S.A., Degtyarev, K.E., Rubtsov, V.I., 1997. Northern Tien Shan: main stages of geodynamic evolution. Geotectonics 31, 445–462.
Miyashiro, A., 1973. The Troodos ophiolitic complex was probably formed in an island arc. Earth Planet Sci. Lett. 19, 218–224.
Nakamura, N., 1974. Determination of REE, Ba, Fe, Mg, Na and K in carbonaceous and ordinary chondrites. Geochem. Cosmochim. Acta 38, 757–775.
Osmonbetov, K.O., Knauf, V.I., 1982. Stratified and Intrusive Formations of Kyrgyzia. vols. 1 and 2. Yilim Publishing House, Frunze, Kyrgyz SSR (in Russian).
Nikolaev, V.A., 1933. About principal structural line of Tianshan. Proceedings of All-Russian Mineralogical Society, Series 2 (62), 347–354 (in Russian).
Pearce, J.A., 2008. Geochemical fingerprinting of oceanic basalts with applications to ophiolite classification and the search for Archean oceanic crust. Lithos 100, 14–48.
Pearce, J.A., Harris, N.B., Tindle, A.G., 1984. Trace element discrimination diagrams for the tectonic interpretation of granitic rocks. J. Petrol. 25–4, 956–983.
Pearce, J.A., Peate, D.W., 1995. Tectonic implications of the composition of volcanic arc magmas. Annu. Rev. Earth Planet Sci. 23, 251–285.
Popov, V.I., 1938. History if Depressions and Uplifts of the Western Tien Shan. Committee of Sciences of UzSSR Publishing House, Tashkent, p. 415 (in Russian).
Qian, Q., Gao, J., Klemd, R., He, G.Q., Song, B., Liu, D.N., Xu, R.H., 2009. Early Paleozoic tectonic evolution of the Chinese South Tianshan Orogen: constraints from SHRIMP zircon U–Pb geochronology and geochemistry of basaltic and dioritic rocks from Xiate, NW China. Int. J. Earth Sci. 98, 551–569.
Rapp, R.P., Shimizu, N., Norman, M.D., Applegate, G.S., 1999. Reaction between slab derived melts and peridotite in the mantle wedge: experimental constraints at 3.8 GPa. Chem. Geol. 160, 335–356.
Richards, J., Kerrich, R., 2007. Special paper: adakite-like rocks: their diverse origins and questionable role in metallogenesis. Econ. Geol. 102, 1–40.
Rojas-Agramonte, Y., Kröner, A., Alexeiev, D.V., Jeffreys, T., Khudoley, A.K., Wong, J., Geng, H., Shu, L., Semiletkin, S.A., Mikolaichuk, A.V., Kiselev, V.V., Seltmann, R., 2014. Detrital and igneous zircon ages for supracrustal rocks of the Kyrgyz Tianshan and implications for crustal growth in the southern Central Asian Orogenic Belt. Gondwana Res. 26, 957–974.
Ryazantsev, A.V., Degtyarev, K.E., Kotov, A.B., Sal'nikova, E.B., Anisimova, I.V., Yakovleva, S.Z., 2009. Ophiolite sections of the Dzhalair-Nayman zone, South Kazakhstan: their structure and age substantiation. Dokl. Earth Sci. 427A, 902–906.
Safonova, I., Kotlyarov, A., Krivonogov, S., Xiao, W., 2017. Intra-oceanic arcs of the Paleo-Asian Ocean. Gondwana Res. 50, 167–194.
Schiano, P., Monzier, M., Eissen, J.P., Martin, H., Koga, K.T., 2010. Simple mixing as the major control of the evolution of volcanic suites in the Ecuadorian Andes. Contrib. Mineral. Petrol. 160 (2), 297–312.
Seltmann, R., Armstrong, R., Dolgopolova, A., Yakubchuk, A., Konopelko, D., Creaser, R.A., Morelli, R., Zhang, X., Chen, C., 2008. Granitic magmatism and related mineralization in the altaids: case study from the Tienshan mineral belt. In: 18th Annual V.M. Goldschmidt Conference, Vancouver, Canada. Goldschmidt Conference Abstracts, A846.
Seltmann, R., Konopelko, D., Biske, G., Divaev, F., Sergeev, S., 2011. Hercynian postcollisional magmatism in the context of Paleozoic magmatic evolution of the Tien Shan orogenic belt. J. Asian Earth Sci. 42, 821–838.
Şengör, A.M.C., Natal'in, B.A., Burtman, V.S., 1993. Evolution of the Altaid tectonic collage and Paleozoic crust growth in Eurasia. Nature 364, 299–307.
Sun, S.S., McDonough, W.F., 1989. Chemical and isotopic systematic of oceanic basalts; implications for mantle composition and processes. In: Saunders, A.D., Norry, M.J. (Eds.), Magmatism in the Ocean Basins, vol. 42. Geological Society of London, Special Publications, pp. 313–345.
Tagiri, M., Yano, T., Bakirov, A., Nakajima, T., Uchiumi, S., 1995. Mineral parageneses and metamorphic P–T paths of UHP eclogites from Kyrgyzstan Tien-Shan. Isl. Arc 4, 280–292.
Thorkelson, D.J., Breitsprecher, K., 2005. Partial melting of slab window margins: genesis of adakitic and non-adakitic magmas. Lithos 79, 25–41.
Tursungaziev, B.T., Petrov, O.V., 2008. Geological Map of Kyrgyz Republic. VSEGEI, Sankt-Petersburg scale 1:500000 (in Russian).

Wang, T., Jahn, B.M., Kovach, V.P., Tong, Y., Hong, D.W., Han, B.F., 2009. Nd-Sr isotopic mapping of the Chinese Altai and implications for continental growth in the Central Asian Orogenic Belt. Lithos 110 (1–4), 359–372.
Wang, M., Zhang, J.J., Zhang, B., Qi, G.W., 2015. An Early Paleozoic collisional event along the northern margin of the Central Tianshan Block: constraints from geochemistry and geochronology of granitic rocks. J. Asian Earth Sci. 113, 325–338.
Windley, B.F., Alexeiev, D., Xiao, W., Kröner, A., Badarch, G., 2007. Tectonic models for accretion of the central Asian orogenic belt. J. Geol. Soc. Lond. 164, 31–47.
Xiao, W.J., Windley, B.F., Allen, M., Han, C.M., 2013. Paleozoic multiple accretionary and collisional tectonics of the Chinese Tianshan orogenic collage. Gondwana Res. 23, 1316–1341.
Zheng, R., Li, J., Zhang, J., Xiao, W., Wang, Q., 2020. Permian oceanic slab subduction in the southmost of Central Asian Orogenic Belt: evidence from adakite and high-Mg diorite in the southern Beishan. Lithos 358–359, 105406.
Zonenshain, L.P., Kuzmin, M.I., Natapov, L.M., 1990. Geology of the USSR: A Plate-Tectonic Synthesis. American Geophysical Union, Washington, DC, p. 242.